OceanDynamics manuscript No.
(will be inserted by the editor)

Modelling the impact of ocean warming on melting and water masses of ice shelves in the Eastern Weddell Sea

Malte Thoma[1,2], Klaus Grosfeld[2], Keith Makinson[3], Manfred A. Lange[4]

[1] Bayerische Akademie der Wissenschaften, Kommission für Glaziologie, 80539 München, Germany
[2] Alfred Wegener Institute for Polar and Marine Research (AWI), Bussestrasse 24, 27570 Bremerhaven, Germany, e-mail: Malte.Thoma@awi.de
[3] British Antarctic Survey (BAS), High Cross, Madingley Road, Cambridge, CB3 0ET, United Kingdom
[4] Energy, Environment and Water Research Center (EEWRC), The Cyprus Institute, P.O. Box 27456, CY-1645 Nicosia, Cyprus

January 6, 2010

Abstract The Eastern Weddell Ice Shelves (EWIS) are believed to modify the water masses of the coastal current and thus preconditions the water mass formation in the southern and western Weddell Sea. We apply various ocean warming scenarios to investigate the impact on the temperature–salinity distribution and the sub-ice shelf melting in the Eastern Weddell Sea. In our numerical experiments the warming is imposed homogeneously along the open inflow boundaries of the model domain, leading to a warming of the Warm Deep Water (WDW) further downstream. Our modelling results indicate a weak quadratic dependence of the melt rate at the ice shelf base on the imposed amount of warming, which is consistent with earlier studies. The total melt rate has a strong dependence on the applied ocean warming depth. If the warming is restricted to the upper ocean (above 1000 m), the water column (aside from the mixed surface layer) in the vicinity of the ice shelves stabilises. Hence, reduced vertical mixing will reduce the potential of Antarctic Bottom Water formation further downstream with consequences on the global thermohaline circulation. If the warming extends to the abyss, the WDW core moves significantly closer to the continental shelf break. This sharpens the Antarctic Slope Front and leads to a reduced density stratification. In contrast to the narrow shelf bathymetry in the EWIS region, a wider continental shelf (like in the southern Weddell Sea) partly protects ice shelves from remote ocean warming. Hence, the freshwater production rate of, e.g., the Filchner Ronne Ice Shelf increases much less compared to the EWIS for identical warming scenarios. Our study therefore indicates that the ice-ocean interaction has a significant impact on the temperature-salinity distribution and the water column stability in the vicinity of ice shelves located along a narrow continental shelf. The effects of ocean warming and the impact of increased freshwater fluxes on the circulation are of the same order of magnitude and superimposed. Therefore, a consideration of this interaction in large-scale climate studies is essential.

Key words Weddell Sea – Ocean warming – Numerical ocean modelling – Ice-ocean interaction – Brunt Ice Shelf – Riiser-Larsen Ice Shelf – Antarctica

1 Introduction

The Weddell Sea is known as one of the most productive regions of deep and bottom water in the world ocean (e.g., Fahrbach et al., 1995, 2001). Besides the North Atlantic, it is the most important region driving the global thermohaline circulation (e.g., Goosse and Fichefet, 1999). Therefore, climate-change-induced modifications of the water masses in this region will most probably have an impact on remote sites (e.g., Swingedouw et al., 2008). The abrupt disintegration of the Larsen A and B Ice Shelves (LIS) (e.g., Rott et al., 1996; Scambos et al., 2000; MacAyeal et al., 2003) in the western Weddell Sea (Figure 1) during the mid 1990's and in 2002, respectively, led to an accelerated discharge of the Antarctic Peninsula ice streams (Rignot et al., 2004; Scambos et al., 2004). One of the most probable reasons for this disintegration is atmospheric warming, leading to

melt ponds and surface water intrusion into ice shelf fissures during summer, followed by bursting during freezing in winter time (e.g., Scambos et al., 2000; Vaughan et al., 2003). On the other hand, Shepherd et al. (2003) suggest a leading role of basal melting induced by ocean circulation. Upwelling of warm deep waters through deep troughs on the continental shelf and associated flooding of the ice shelf cavities leads to increased basal melting. This preconditions the ice shelf for probable atmospherically forced disintegration. In this context Lange et al. (2005) simulated the net freshwater flux by basal melting of Larsen C from ocean and ice dynamic modelling, indicating a substantial contribution to the Weddell Sea freshwater budget from this comparatively small ice-shelf region.

The other major ice shelves in the Weddell Sea (Figure 1) are too far south to be affected by the present global atmosphere warming trend within the next decades (Vaughan and Spouge, 2002). However, observations show that ocean warming seems to be responsible for an accelerated discharge of ice into the Amundsen Sea where the mean basal melt rate exceeds 10 m/a (e.g. Jacobs et al., 1996; Jenkins et al., 1997; Hellmer et al., 1998; Rignot et al., 2002; Shepherd et al., 2004; Payne et al., 2007). These exceptionally high melt rates in the Amundsen Sea are caused by Circumpolar Deep Water, flooding the continental shelf. Whether this will destabilise the West Antarctic Ice Sheet itself is still a matter of debate (e.g., Oppenheimer, 1998; Vaughan and Spouge, 2002; Thoma et al., 2008).

In the Eastern Weddell Sea, the mean basal melt rate of ice shelves is only about 0.67 to 1.65 m/a (Thoma et al., 2006a), but ice fronts occasionally overhang the continental shelf break. Along this continental shelf, the Warm Deep Water (WDW) is channeled within the Antarctic Coastal Current. Hence, these ice shelves are expected to be influenced by WDW warming. According to modelling studies, the freshwater production of the Eastern Weddell Ice Shelves (EWIS) is comparable to that of the fourfold bigger Filchner-Ronne Ice Shelf (Timmermann et al., 2001; Hellmer, 2004). Thoma et al. (2006a) showed that the EWIS region is important for the preconditioning of water masses before they pass the Filchner-Ronne shelf and enter the south-western Weddell Sea where deep and bottom water is formed (Gill, 1973; Fahrbach et al., 1995). In various model scenarios Thoma et al. (2006a) demonstrate that the ocean temperatures southwest and downstream of the ice shelves differ by about 1.4°C for the extreme *closed-cavity* scenario and the *removed-ice-shelf* scenario in the Eastern Weddell Sea.

Observations indicate that the meltwater, produced at the base of the EWIS, freshens the topmost ocean layers and therefore stabilises the water column, such that deep and bottom water formation is suppressed (Fahrbach et al., 1994). Hence, climate changes leading to ocean warming will increase the freshwater production in the Eastern Weddell Sea and will also result in less sea ice production. Both processes would therefore further stabilise the water column in this region. On the other hand, any modification of the ice shelf geometry and its consequences on the water masses would probably lead to a water column destabilisation (Thoma et al., 2006a). The question dealt with in this paper is, how much rising ocean temperatures would increase basal melting (assuming that the geometry and extent of the ice shelf is not affected).

2 Experimental setup

The numerical ocean model used in this study has been described in detail by Thoma et al. (2006a); here we only refer to the boundary and forcing conditions. The model domain covers the Weddell Sea from 40°W to 0° and 78°S to 66°S (Figure 1) and is forced with (a) a climatological monthly wind field (Kottmeier and Sellmann, 1996), (b) prescribed vertically integrated mass transport stream function values along the open boundaries at the western, northern, and eastern model domain (Thoma et al., 2006a), (c) restoring of temperature and salinity to observations at the lateral open boundaries (Gouretski et al., 1999; Fahrbach et al., 2004), and (d) surface restoring of temperature and salinity according to reasonably adjusted observations (Gouretski et al., 1999; Thoma et al., 2006a). The simplified surface restoring, applied instead of a coupled sea ice model, allows us to investigate the mere impact of warmed ocean waters onto the cavity's freshwater production rate, assuming fixed atmospheric conditions. The freshwater fluxes in the ice-shelf cavities are calculated with a three-equation scheme, based on the pressure-depending freezing point as well as on the conservation of heat and salinity (e.g., Holland and Jenkins, 1999). The spin-up of the model from initial conditions takes about 11 years of integration until a quasi steady state is reached (Figure 2). The control run presented in Thoma et al. (2006a), used as reference in this work, is derived from averaged values of the following 19 years. After 30 years of

model integration nine warming scenarios (listed in Table 1 and discussed below) are applied in which we increase the ocean temperature along the prime meridian, coinciding with the eastern boundary of the model domain. In this area, the Antarctic Coastal Current (as part of the Weddell Gyre) enters the Weddell Sea. Scenario $\mathcal{S}_{0.1}^{10y}$ is featured by a temperature increase of 0.1°C, evenly distributed over 10 years. This scenario is based upon observations by Robertson et al. (2002), Fahrbach et al. (2004), and Smedsrud (2005), who described a 0.01°C increase per year along the prime meridian by means of hydrographic stations and mooring data. However, the articles are nonuniform with respect to the warming depth. This data also indicates that ocean warming is not necessarily compensated by a change in salinity; hence we kept the salinity boundary conditions constant. Other warming scenarios (Scenarios $\mathcal{S}_{0.5}^{10y}$ & $\mathcal{S}_{1.0}^{10y}$), are based on Intergovernmental Panel on Climate Change (IPCC) emission scenarios and general circulation model studies by Manabe and Stouffer (1994) and O'Farrell et al. (1997) who discuss atmospheric warming as a response to CO_2 increase. Grosfeld and Sandhäger (2004) took these results as motivation for a 0.5°C warming scenario for Weddell Sea water masses in an idealized coupled ice shelf-ocean modelling effort. Here, we apply a 0.5°C and a 1.0°C warming scenario (ramped up over 10 years) indicated as $\mathcal{S}_{0.5}^{10y}$ and $\mathcal{S}_{1.0}^{10y}$, respectively (Table 1). Three somewhat more unrealistic scenarios ($\mathcal{S}_{0.1}^{inst}$, $\mathcal{S}_{0.5}^{inst}$, and $\mathcal{S}_{1.0}^{inst}$) are designed to compare the up-to-now dilatory temperature increase with a sudden temperature jump of about the same amount. In all aforementioned cases, only the upper 1000 m of the water column along the prime meridian are warmed, similar to the findings of Manabe and Stouffer (1994) and the most recent IPCC report (IPCC, 2007), which indicate that the warming does not reach the deep ocean yet. However, with time any change of the upper ocean temperature may propagate to the deep ocean as well. Hence, we define the scenarios ${}^{a}\mathcal{S}_{0.1}^{inst}$ and ${}^{a}\mathcal{S}_{0.5}^{inst}$ in which the complete water column down to the abyss is evenly warmed by 0.1°C and 0.5°C, respectively. Finally, the artificial scenario $\tilde{\mathcal{S}}_{1.0}^{inst}$ is identical to $\mathcal{S}_{1.0}^{inst}$, but without any ice-ocean interaction. Hence, no meltwater is released from the EWIS to the ocean, which allows us to study the impact of ocean warming alone in more detail.

3 Results

3.1 Fresh water flux

Thirteen years after warming is induced, the model's equilibriums are obtained. Figure 3 shows the freshwater flux produced by the EWIS for different warming scenarios. Instantaneous temperature rises after 30 model years lead to transient oscillations of the freshwater flux for some years; ramped temperature rises are completed in model year 40. We compare long-term averages of the freshwater flux from model year 43 to 60 after transition effects have adequately faded out and a quasi-steady state is reached. The long-term mean of the control run (years 10 to 30) of about 2.10 mSv (equivalent to a basal melt rate of 0.88 m/a, which for an ice shelf base of 7.5×10^3 km^2 results in a mass loss of 66.4 km^3/a, Thoma et al., 2006a) is increased by 4% to 97%, depending on the warming scenario (Table 1). Although the total energy increase provided by the warming scenario ${}^{a}\mathcal{S}_{0.1}^{inst}$ is significantly lower than those of $\mathcal{S}_{0.5}^{inst}$ and $\mathcal{S}_{0.5}^{10y}$, the total freshwater increase by ice shelf melting is nearly identical. This indicates that the warming depth alters the ocean dynamics (see Section 3.2 for details). The differences between ramped ($\mathcal{S}_{x}^{10y}$) and sudden ($\mathcal{S}_{x}^{inst}$) temperature rises are negligible after the quasi steady state is reached with respect to basal mass balance, temperature, and salinity distribution. From the numerical point of view, this response indicates that the model is stable with respect to the applied warming scenarios. From the physical point of view, this indicates a short residence time of the cavity water masses in this region of Antarctica, as a remote ocean warming leads to an increased melting, instantaneously. Therefore, we confine ourselves to the instant-warming scenarios ($\mathcal{S}_{x}^{inst}$) in the following discussion.

3.2 Impact of warming

The temperature and salinity distribution at 300 m depth in the control run and the final state for scenario $\mathcal{S}_{0.5}^{inst}$ are shown in Figure 4. Warmer water masses enter the model domain at the eastern boundary (compare Figure 4a and b) and spread throughout the model domain. Only the shallower continental shelf in the south-western model domain is nearly unaffected. The continental shelf break prevents the warmer water masses from continuing southwards. Even within the deep

Filchner trough (an up to 1000 m deep depression in front of the Filchner ice shelf) the warming is negligible (not shown). Less pronounced, but visible, is the impact on the salinity distribution due to temperature-induced modifications in the flow regime: Comparing Figures 4c and d reveals that the warming results in a redistribution of salinity and its increase further downstream in the central Weddell Sea approximately along 71°S.

More detailed information about the warming impact on the hydrography in the vicinity of the EWIS can be obtained from cross sections along a track after the water masses have passed most parts of the ice shelves (Figure 1). Figure 5 shows temperature, salinity, and density of the control run and the final states of scenarios $\mathcal{S}^{\text{inst}}_{1.0}$ and ${}^{\text{a}}\mathcal{S}^{\text{inst}}_{0.5}$. From the two different model set-ups (warming of the upper ocean only and warming to the abyss) we choose always the one with the strongest warming, where the magnitude of the impacts on the water mass properties as well as on the basal melt rate is largest. In this area, about 1000 km downstream of the applied warming along the prime meridian, its impact on water masses is studied. Arrow $\mathcal{A}$ in Figure 2 symbolises the difference between the warming scenarios and the control run as shown in Figure 6. This figure highlights the impact of ocean warming on the water column by showing anomaly plots for scenarios $\mathcal{S}^{\text{inst}}_{1.0}$ and ${}^{\text{a}}\mathcal{S}^{\text{inst}}_{0.5}$, respectively.

Comparing the results of the control run and $\mathcal{S}^{\text{inst}}_{1.0}$ (Figures 5a–f and 6a–c) reveals that the deep and near surface ocean water masses are barely modified by the warming induced at the eastern model boundary down to 1000 m. Note that the cavity's temperature near the ice front is also only slightly increased. The additional heat provided to the cavity is converted into cold meltwater and leads to significant freshening (Figure 6b). The most pronounced temperature impact 1000 km downstream of the induced warming takes place in the WDW core (Figure 6a), which is about 0.6°C warmer, leading to stronger temperature gradients in all directions. Although the boundary conditions for salinity have not been altered, a rise of the WDW salinity is also observed (Figure 6b). However, this salinity increase is not able to compensate the temperature effect on the density; hence, the overall impact of the warming results in a density decrease between 200 m and 2000 m, yielding to a more stabilised water column (Figure 6c).

If the water column is warmed to the abyss (${}^{\text{a}}\mathcal{S}^{\text{inst}}_{0.5}$, Figures 5g–i and 6d–f), the strongest impact can still be observed in the WDW-core, warmed by 0.5°C in this case, which is the same amount as the temperature increase about 1000 km upstream. Simultaneously the WDW-core moves about 150 km closer to the shelf break as a consequence of the Weddell Gyre's dynamic response to the altered temperature field. The barotropic transport (not shown) increases in all warming scenarios and dynamically pushes the Antarctic Slope Front outwards, closer to the shelf break (Núñez-Riboni and Fahrbach, 2009). Hence, the Antarctic Slope Front is more pronounced, and the cavity is flushed with warmer water masses, leading to the massive freshwater increase shown in Figure 3 and Table 1. In addition to this strong impact on cavity water masses, the deep water masses at the shelf break are modified as well. Salinity is affected in a much wider range than for the depth-limited warming; hence, the impact on the density is different: The upper water masses become denser, while bottom water masses on the deep continental slope become lighter. Therefore, the stability of the water column is reduced.

3.3 Impact of ice-ocean interaction

The modelled salinity decrease within the cavity is expected as a consequence of increased melting for all warming scenarios. In contrast to this, there seems to be no explanation for the salinity decrease on the continental slope around 1500 m depth (for the depth-limited warming scenarios, Figure 6b) or 3000 m depth (for the abyssal warmed scenarios, Figure 6e), respectively. Fresher water masses, produced in the cavity, are expected to rise to the surface and should not flow down the continental slope. In order to determine the cause of this significant freshening in the deeper ocean, we run an additional, artificial scenario $\tilde{\mathcal{S}}^{\text{inst}}_{1.0}$, in which the ice-ocean interaction is suppressed and consequently no freshwater production at the ice-shelf base occurs.

Figure 7a-c shows the temperature, salinity, and density anomalies between the final state of $\tilde{\mathcal{S}}^{\text{inst}}_{1.0}$ and the corresponding "control run", indicated as arrow $\mathcal{B}$ in Figure 2. The model shows a warming-induced detachment of the WDW core from the shelf along with a significant salinity reduction between about 300 m and 2000 m. This freshening signal can be seen up to about 300 km from the coast. Salinity is the governing quantity with respect to density in the Southern Ocean. Ignoring the seasonally driven upper ocean layer (above about 200 m), this density reduction at intermediate depth stabilise the whole water column (Figure 7c).

Additionally, Figure 7d-f shows the difference between the two final states of scenarios $\mathcal{S}_{1.0}^{\text{inst}}$ and $\tilde{\mathcal{S}}_{1.0}^{\text{inst}}$, indicated by arrow $\mathcal{C}$ in Figure 2, and hence the effect of meltwater production. The main impact of this freshwater production takes place at the ice shelf base, where freshening and cooling occurs. The density modification is principally confined to the cavity (Figure 7f), but the displacement of unmodified water masses in the open ocean also results in a slight density increase. Since cooling and freshening have opposing effects on the density, the meltwater signal (Figure 7d-e) can be traced further offshore than the density signal (Figure 7f) itself. Also, the impact of meltwater production ($\mathcal{C}$, Figure 7d-f) is partly the reverse of that of ocean warming ($\mathcal{B}$, Figure 7a-c), and these two effects superimpose ($\mathcal{A} = \mathcal{B} \cup \mathcal{C}$), resulting in the effects shown in Figure 6a-c.

4 Summary and Conclusion

From the warming scenarios presented in this study we conclude that the homogeneously induced warming along the prime meridian, coinciding with the eastern model boundary, is mainly constrained further downstream to the WDW core in the Weddell Sea, even if the whole water column is warmed. The results are independent of the warming rate, but depend on the final temperature rise as well as on the depth to which the warming extends. The overall impact of ocean warming can be split into two separate effects: a warming-induced part and an increased freshwater production part, both modifying ocean dynamics. Both effects superimpose in the vicinity of ice shelves. The warming-induced part does not only affect the temperature distribution within the ocean, but the salinity structure, too. The missing meltwater signal at the shelf break smooths the Antarctic Slope Front by flattening the density gradient perpendicular to the coast. Hence, the barotropic transport decreases and as a result the WDW core moves away from the coast if ice-ocean interaction is neglected.

The effect on stratification, and therefore the stability of the water column, strongly depends on the depth to which ocean warming takes place: If only the upper ocean is warmed, the intermediate water masses between about 100 m and 2000 m become less dense, hence vertical mixing becomes less likely. If, on the other hand, the water column is warmed down to the abyss, the salinity redistribution results in a distinct density increase of the WDW core, while deeper water masses on the continental slope become less dense. Assuming the seasonal density increase of surface waters due to sea ice production (Gordon, 1978) is still sufficient to mix these water masses down to intermediate depths, deep vertical mixing and therefore the production of deep and bottom waters would become more likely.

The impact on the basal mass balance of the EWIS depends strongly on the warming depth: Figure 8 shows that if warming is limited to the upper 1000 m, the melting increases far less compared to those scenarios where the water is warmed down to the abyss. The dependence of the melting on the amount of temperature increase, indicated in Figure 8, can be fitted with a quadratic function. This is in consistence with the study of Holland et al. (2008), based on idealized ice shelf geometries. The strong impact of ocean warming on the basal mass balance of EWIS results from the lack of a wide continental shelf (a *type-2* ice shelf according to Beckmann and Goosse, 2003), which could protect EWIS from a warmed Antarctic Coastal Current. The *type-1* Filchner-Ronne Ice Shelf, which is separated by a 400 km wide continental shelf from warmer WDW water masses, is less prone to ocean warming. This has been modelled in a complementary study by Thoma et al. (2006b) applying the warming scenario $\mathcal{S}_{0.5}^{\text{inst}}$ to a much larger domain, covering the whole Weddell Sea. The black triangle in Figure 8, adapted from Thoma et al. (2006b), indicates the significantly lesser sensitivity of the *type-1* Filchner Ronne Ice Shelf (FRIS) to ocean warming.

The spatial distribution of the increased basal melting is indicated in Figure 9 for the most extreme scenarios $\mathcal{S}_{0.5}^{\text{inst}}$ and ${}^{\text{a}}\mathcal{S}_{0.5}^{\text{inst}}$. The areas most vulnerable to increased ocean temperatures are the exposed ice shelf front as well as the areas where ice streams formed deep troughs. In particular the increased melting close to the grounding line may have implications for the dynamics of the whole ice shelf as well as on the ice sheet in the hinterland.

With the weak ocean warming, observed at present, it will take several decades until ice shelves in the Eastern Weddell Sea will show a significant geometry change as reaction on increased bottom melting. However, a modified ice shelf geometry will have feedbacks on the oceanic circulation and the basal melt pattern as well (Grosfeld and Sandhäger, 2004). Hence, future modelling studies dealing with ocean warming in the Southern Ocean should include a coupled ice-shelf ocean component.

Acknowledgements This work is part of the German CLIVAR/marin-project. Founding by the Bundesministerium für Bildung, Wissenschaft, Forschung und Technologie (bmb+f) der Bundesrepublik Deutschland, contract 03F0377C, is gratefully acknowledged. The authors wish to thank Povl Abrahamsen for the recovery of some lost data, Andrea Bleyer for proof reading as well as Hartmut Hellmer, Angelika Humbert and three anonymous reviewers for helpful suggestions which improved the manuscript.

References

Beckmann, A., Goosse, H., 2003. A parametrization of ice shelf - ocean interaction for climate models. Ocean Modelling 5, 157–170.

Fahrbach, E., Harms, S., Rohardt, G., Schröder, M., Woodgate, R. A., February 2001. Flow of bottom water in the northwestern Weddell Sea. J. Geophys. Res. 106 (C2), 2761–2778.

Fahrbach, E., Hoppema, M., Rohardt, G., Schröder, M., Wisotzki, A., 2004. Decadal-scale variations of water mass properties in the deep Weddell Sea. Ocean Dynamics 54, 77–91.

Fahrbach, E., Peterson, R. G., Rohardt, G., Schlosser, P., Bayer, R., 1994. Suppression of bottom water formation in the southeastern Weddell Sea. Deep-Sea Res. 41 (2), 389–411.

Fahrbach, E., Rohardt, G., Scheele, N., Schröder, M., Strass, V., Wisotzki, A., 1995. Formation and discharge of deep and bottom water in the nortwestern Weddell Sea. J. Mar. Res. 53 (4), 515–538.

Gill, A. E., 1973. Circulation and bottom water mass formation in the Weddell Sea. Deep-Sea Res. 20, 111–140.

Goosse, H., Fichefet, T., 1999. Importance of ice-ocean interactions for the global ocean circulation: A model study. J. Geophys. Res. 104 (C10), 23337–23355.

Gordon, A. L., 1978. Deep Antarctic convection west of Maud Rise. J. Phys. Oceanogr. 8, 600–612.

Gouretski, V., Jancke, K., Reid, J., Swift, J., Rhines, P., Schlitzer, R., Yashayaev, I., 1999. WOCE Hydrographic Programme Special Analysis Centre, Atlas of Ocean Sections. CD-ROM.

Grosfeld, K., Sandhäger, H., 2004. The evolution of a coupled ice shelf – ocean system under different climate states. Global Planet. Change 42, 107–132, doi:10.1016/j.gloplacha.2003.11.04.

Hellmer, H. H., 2004. Impact of Antarctic ice shelf basal melting on sea ice and deep ocean properties. Geophys. Res. Lett. 31, 1–4, L10307, doi:10.1029/2004GL019506.

Hellmer, H. H., Jacobs, S. S., Jenkins, A., 1998. Oceanic erosion of a floating Antarctic glacier in the Amundsen Sea. In: Jacobs, S. S., Weiss, R. F. (Eds.), Ocean, Ice, and Atmosphere: Interactions at the Antarctic Continental Margin. Vol. 75 of Antarctic Research Series. Americal Geophysical Union, Washington, D.C., pp. 83–99.

Holland, M. D., Jenkins, A., 1999. Modeling thermodynamic ice-ocean interaction at the base of an ice shelf. J. Phys. Oceanogr. 29, 1787–1800.

Holland, P. R., Jenkins, A., Holland, D. M., 2008. The response of ice shelf basal melting to variations in ocean temperature. J. Climate 21, 2558–2572.

IPCC, 2007. The physical science basis. contribution of working group i to the fourth assessment report of the intergovernmental panel on climate change. In: Solomon, S., Qin, D., Manning, M., Chen, Z., Marquis, M., Averyt, K. B., Tignor, M., Miller, H. L. (Eds.), Climate Change 2007. Cambridge University Press, Cambridge, United Kingdom and New York, NY, USA, p. 1pp.

Jacobs, S. S., Hellmer, H. H., Jenkins, A., 1996. Antarctic ice sheet melting in the Southeast Pacific. Geophys. Res. Lett. 23 (9), 957–960.

Jenkins, A., Vaughan, D. G., Jacobs, S. S., Hellmer, A. H., Keys, J. R., 1997. Glaciological and oceanographic evidence of high melt rates beneath Pine Island Glacier, West Antarctica. J. Glaciol. 43 (143), 114–121.

Kottmeier, C., Sellmann, L., 1996. Atmospheric and oceanic forcing of Weddell Sea ice motion. J. Geophys. Res. 101 (C9), 20809–20824.

Lange, M. A., Blindow, N., Breuer, B., Grosfeld, K., Kleiner, T., Mohrholz, C. O., Nicolaus, M., Oelke, C., Sandhäger, H., Thoma, M., 2005. Numerical model studies of Antarctic ice-sheet – ice-shelf – ocean systems and ice caps. Ann. Glaciol. 41, 111–120.

MacAyeal, D. R., Scambos, T. A., Hulbe, C. L., Fahnestock, M. A., 2003. Catastrophic ice-shelf break-up by an ice-shelf-fragment-capsize mechanism. J. Glaciol. 49 (164), 22–35.

Manabe, S., Stouffer, R. J., 1994. Multiple-century response of a coupled ocean-atmosphere model to an increase of atmospheric carbon dioxide. J. Climate 7, 5–23.

Núñez-Riboni, I., Fahrbach, E., 2009. Seasonal variability of the Antarctic Coastal Current and its driving mechanisms in the Weddell Sea. Deep-Sea Res. 56 (11), 1927–1941.

O'Farrell, S. P., McGregor, J. L., Rotstayn, L. D., Budd, W. F., Zweck, C., Warner, R., 1997. Impact of transient increases in atmospheric CO_2 on the accumulation and mass balance of the Antarctic Ice Sheet. Ann. Glaciol. 25, 137–144.

Oppenheimer, M., 1998. Global warming and the stability of the West Antarctic Ice Sheet. Nature 393, 325–332.

Payne, A. J., Holland, P. R., Shepherd, A. P., Rutt, I. C., Jenkins, A., Joughin, I., 2007. Numerical modeling of ocean-ice interactions under Pine Island Bay's ice shelf. J. Geophys. Res. 112 (C10019), doi: 10.1029/2006JC003733.

Rignot, E., Casassa, G., Gogineni, P., Krabill, W., Rivera, A., Thomas, R., 2004. Accelerated ice discharge from the Antarctic Peninsula following the collapse of Larsen B ice shelf. Geophys. Res. Lett. 31, l18401, doi:10.1029/2004GL020697.

Rignot, E., Vaughan, D. G., Schmeltz, M., Dupont, T., MacAyeal, D., 2002. Acceleration of Pine Island and Thwaites Glaciers, West Antarctica. Ann. Glaciol. 34, 189–194.

Robertson, R., Visbeck, M., Gordon, A. L., Fahrbach, E., 2002. Long-term temperature trends in the deep waters of the Weddell Sea. Deep-Sea Res. 49 (21), 4791–4806.

Rott, H., Skvarca, P., Nagler, T., 1996. Rapid collapse of Northern Larsen Ice Shelf, Antarctica. Science 271 (5250), 788–792.

Scambos, T. A., Bohlander, J. A., Shuman, C. A., Skvarca, P., 2004. Glacier acceleration and thinning after ice shelf collapse in the Larsen B embayment, Antarctica. Geophys. Res. Lett. 31, l18402, doi:10.1029/2004GL020670.

Scambos, T. A., Hulbe, C., Fahnestock, M., Bohlander, J., 2000. The link between climate warming and break-up of ice shelves in the Antarctic Peninsula. J. Glaciol. 46 (154), 516–530, l18402, doi:10.1029/2004GL020670.

Shepherd, A., Wingham, D., Payne, T., Skvarca, P., 2003. Larsen Ice Shelf has progressively thinned. Science 302 (5646), 856–859.

Shepherd, A., Wingham, D. J., Rignot, E., 2004. Warm ocean is eroding West Antarctic Ice Sheet. Geophys. Res. Lett. 31, doi: 10.1029/2004GL021106.

Smedsrud, L. H., 2005. Warming of the deep water in the Weddell Sea along the Greenwich meridian: 1977–2001. Deep-Sea Res. 52, 241–258, doi:10.1016/j.dsr.2004.10.004.

Swingedouw, D., Fichefet, T., Huybrechts, P., Goosse, H., Driesschaert, E., Loutre, M. F., 2008. Antarctic ice-sheet melting provides negative feedbacks on future climate warming. Geophys. Res. Lett. 35 (17).

Thoma, M., Grosfeld, K., Lange, M. A., 2006a. Impact of the Eastern Weddell Ice Shelves on water masses in the eastern Weddell Sea. J. Geophys. Res. 111 (C12010), doi:10.1029/2005JC003212.

Thoma, M., Grosfeld, K., Lange, M. A., 2006b. The impact of ocean warming and ice shelf geometry on the basal melt rate of the FRIS. FRISP Report 17.

Thoma, M., Jenkins, A., Holland, D., Jacobs, S., 2008. Modelling Circumpolar Deep Water intrusions on the Amundsen Sea continental shelf, Antarctica. Geophys. Res. Lett. 35, L18602+.

Timmermann, R., Beckmann, A., Hellmer, H. H., 2001. The role of sea ice in the fresh water budget of the Weddell Sea. Ann. Glaciol. 33, 419–424.

Vaughan, D. G., Marshall, G. J., M., C. W., Parkinson, C., Mulvaney, R., Hodgson, D. A., King, J. C., Pudsey, C. J., J., T., 2003. Recent rapid regional climate warming on the Antarctic Peninsula. Clim. Change 60 (3), 243–274.

Vaughan, D. G., Spouge, J. R., Jan 2002. Risk estimation of collapse of the West Antarctic Ice Sheet. Clim. Change 52, 65–91, doi:10.1023/A:1013038920600.

Scenario	Temperature increase			Energy input	Fresh water
	amount	duration	depth	norm. w.r.t. $\mathcal{S}^{\mathrm{inst}}_{0.1}$	flux increase
$\mathcal{S}^{10\mathrm{y}}_{0.1}$	0.1°C	10 years	≤ 1000 m	1	4%
$\mathcal{S}^{\mathrm{inst}}_{0.1}$	0.1°C	instantly	≤ 1000 m	1	4%
$\mathcal{S}^{10\mathrm{y}}_{0.5}$	0.5°C	10 years	≤ 1000 m	5	17%
$\mathcal{S}^{\mathrm{inst}}_{0.5}$	0.5°C	instantly	≤ 1000 m	5	17%
$\mathcal{S}^{10\mathrm{y}}_{1.0}$	1.0°C	10 years	≤ 1000 m	10	41%
$\mathcal{S}^{\mathrm{inst}}_{1.0}$	1.0°C	instantly	≤ 1000 m	10	41%
$\tilde{\mathcal{S}}^{\mathrm{inst}}_{1.0}$	1.0°C	instantly	≤ 1000 m	10	—
${}^{\mathrm{a}}\mathcal{S}^{\mathrm{inst}}_{0.1}$	0.1°C	instantly	abyss	3.5	15%
${}^{\mathrm{a}}\mathcal{S}^{\mathrm{inst}}_{0.5}$	0.5°C	instantly	abyss	17.3	97%

Table 1 Different warming scenarios mentioned in the text. The additional heat provided along the eastern model boundary is given as normalized energy input with respect to Scenario $\mathcal{S}^{\mathrm{inst}}_{0.1}$. The last column summarises the freshwater flux increase induced by ocean warming, with respect to the reference model (Thoma et al., 2006a).

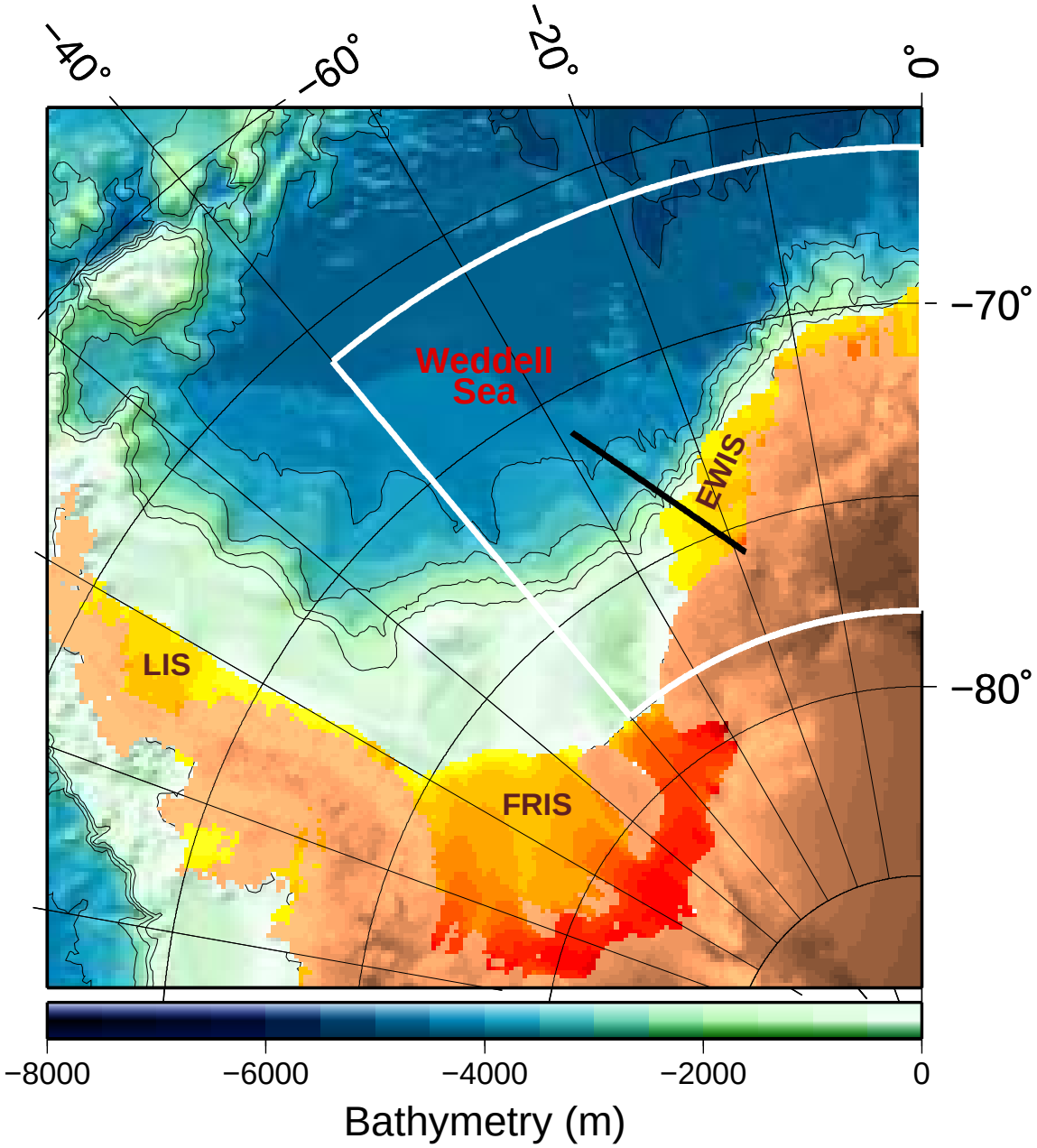

Fig. 1 Location of Larsen (LIS), Filchner-Ronne (FRIS), and Eastern Weddell Ice Shelves (EWIS) in the Weddell Sea, all indicated by yellow (shallow) to red (deep) colours. The white sourrounded area shows the model domain, the solid black line shows the track used for hydrographic cross sections. Inland ice is indicated in brown.

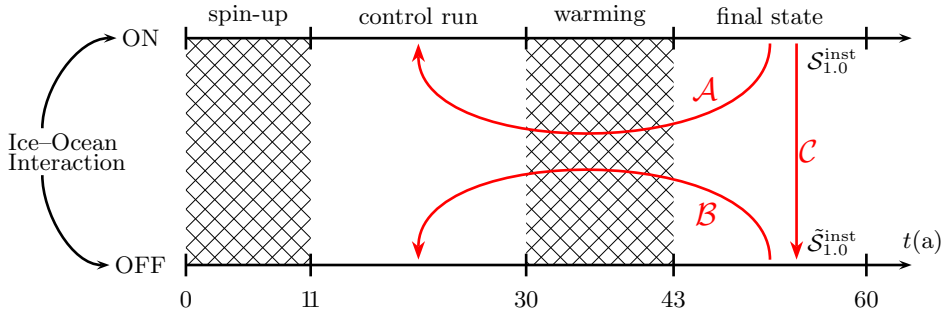

Fig. 2 Time-line of model years. For the discussion of the results, the transient periods until year 11 and between years 30 and 43 are ignored. Arrows indicate differences between scenarios discussed in more detail in the text.

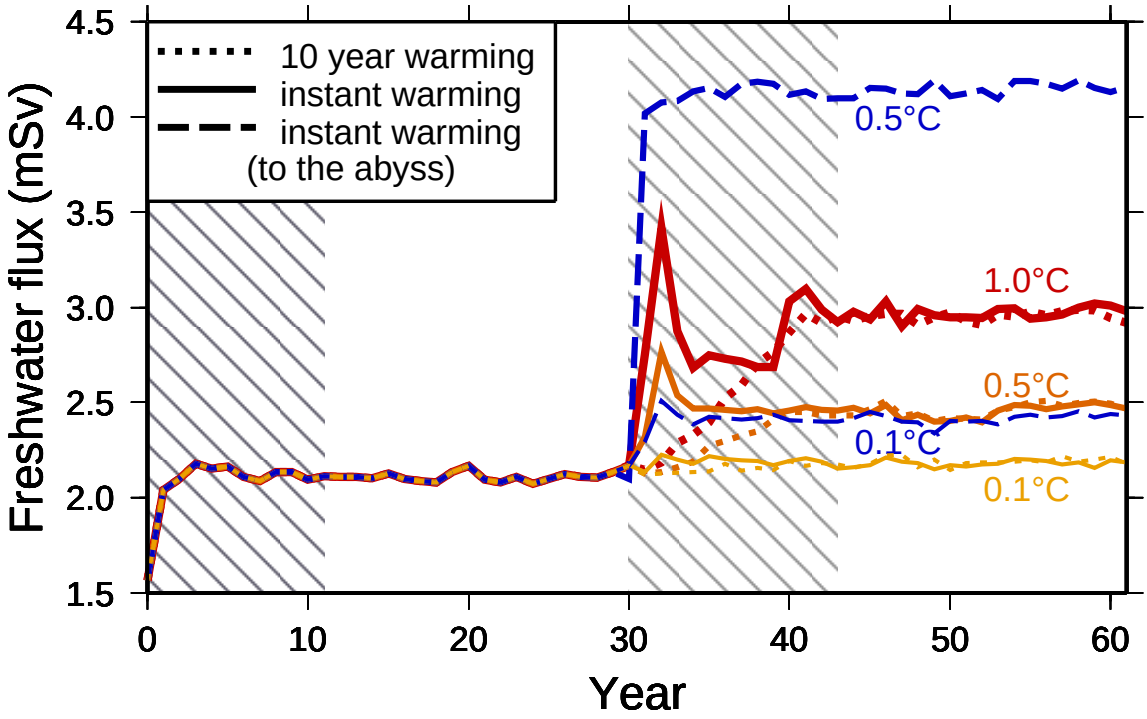

Fig. 3 Calculated annual mean freshwater flux from EWIS ($1\,\mathrm{mSv} = 10^3\,\mathrm{m^3 s^{-1}}$) for different warming scenarios. After about 30 years of integration, ocean warming of indicated temperature is induced. Dotted lines indicate evenly distributed warming during 10 years, solid lines instantaneous warming. The dashed blue lines show the results for the scenarios ${}^{a}\mathcal{S}^{\mathrm{inst}}_{0.1}$ and ${}^{a}\mathcal{S}^{\mathrm{inst}}_{0.5}$, where the water column is warmed instantaneously to the abyss.

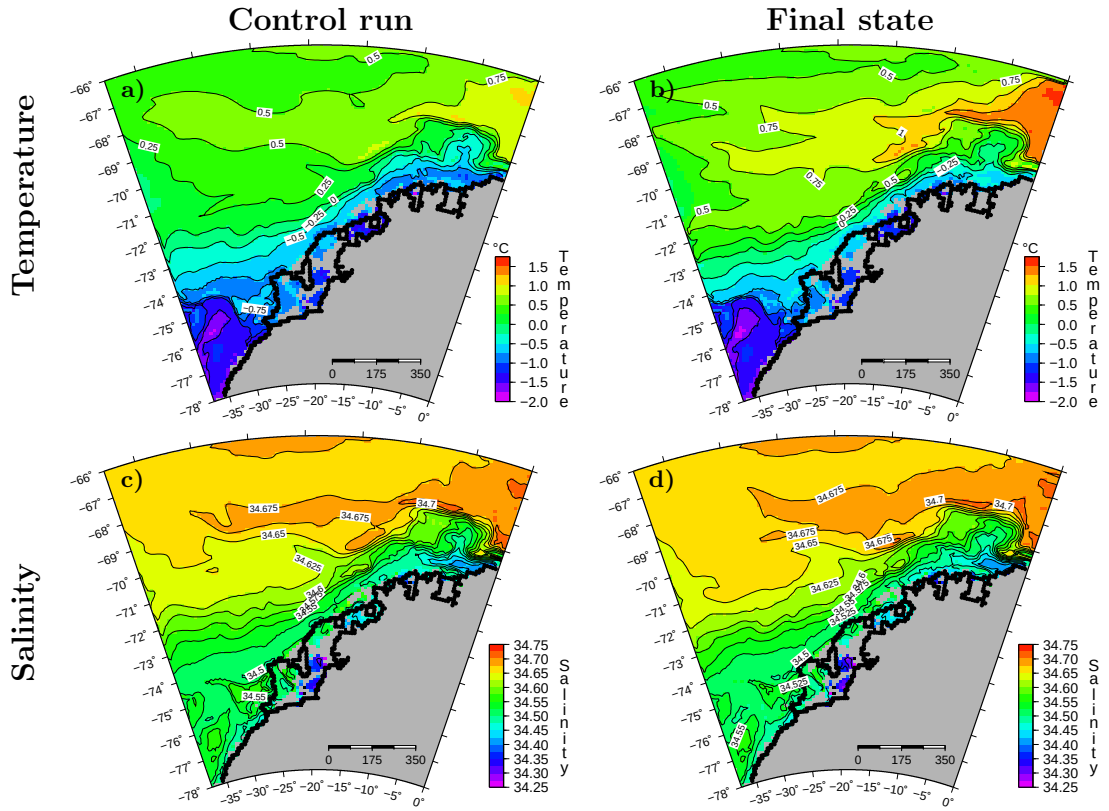

Fig. 4 Temperature (top) and salinity (bottom), at 300 m depth, in the control run (left) and the final state after a 0.5°C warming (right, scenario $\mathcal{S}^{\mathrm{inst}}_{0.5}$). Gray colour indicates bedrock or ice shelf areas.

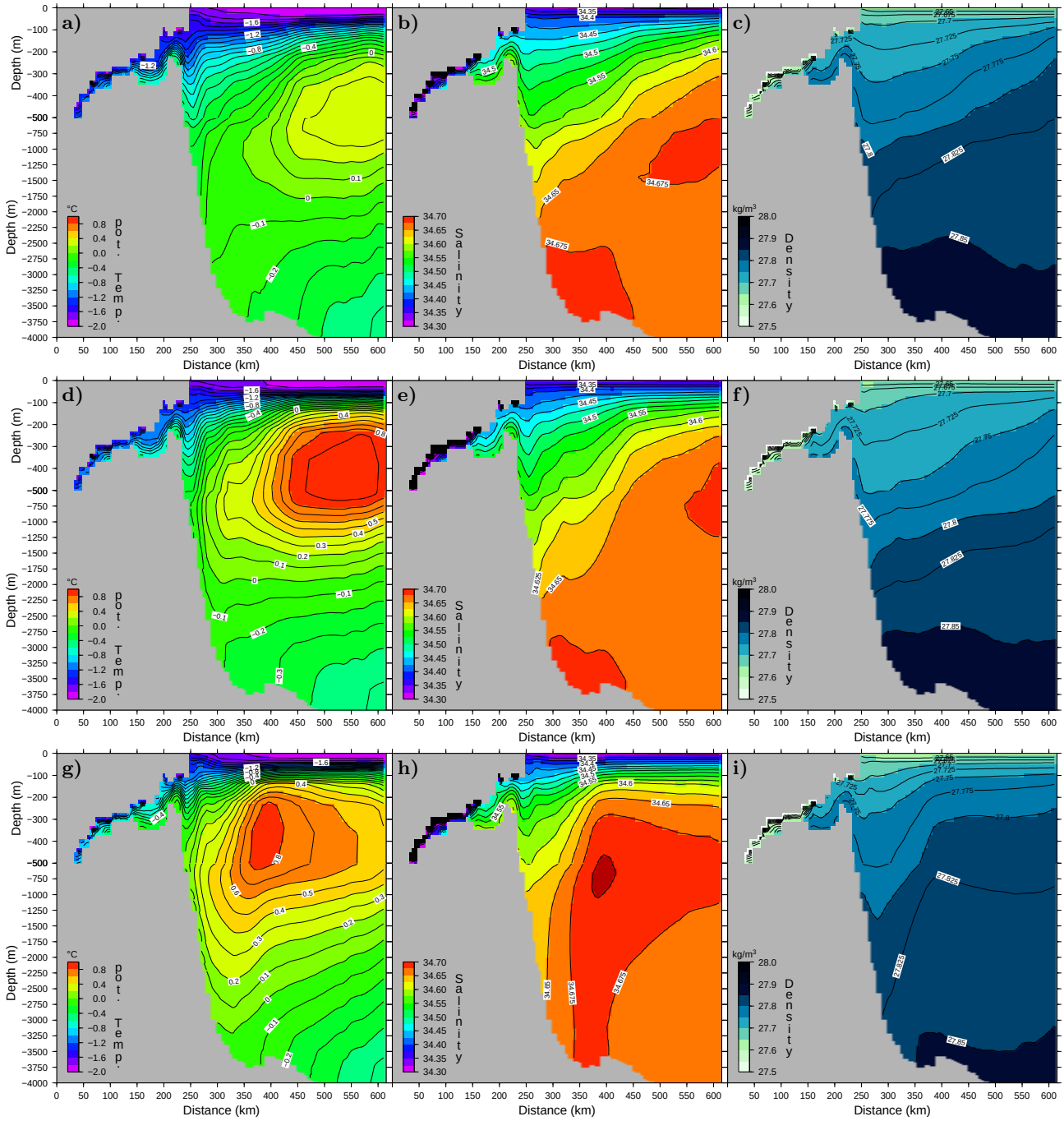

Fig. 5 Temperature (left), salinity (middle), and density (right) along the track shown in Figure 1 for the control run (top) and the final states of scenario $\mathcal{S}^{\text{inst}}_{1.0}$ (middle) and ${}^{\text{a}}\mathcal{S}^{\text{inst}}_{0.5}$ (bottom).

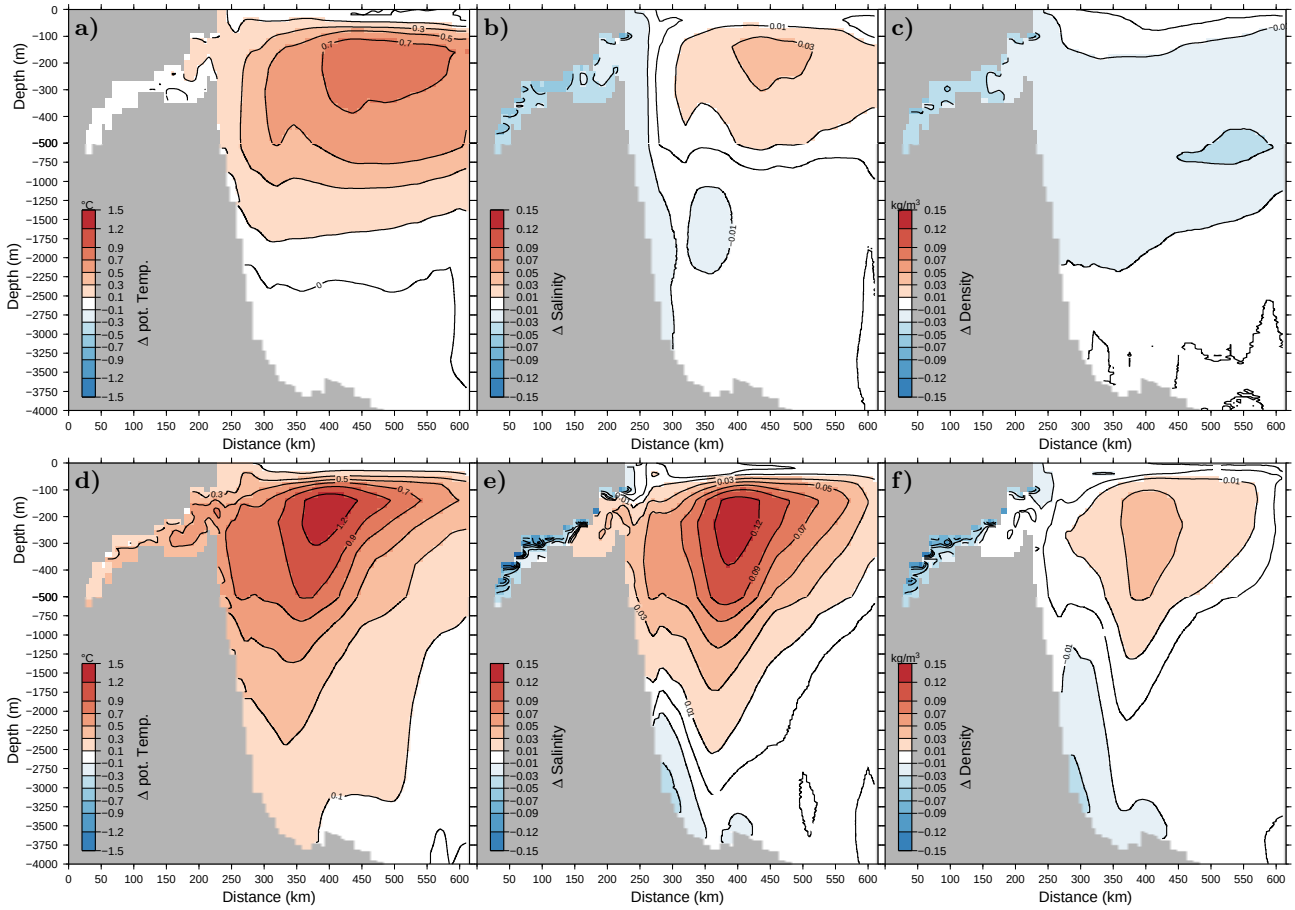

Fig. 6 Differences of temperature (left), salinity (middle), and density (right) between the scenarios $\mathcal{S}^{\text{inst}}_{1.0}$ (a–c) and ${}^{\text{a}}\mathcal{S}^{\text{inst}}_{0.5}$ (d–f) and the control run, respectively. (Corresponds to arrow $\mathcal{A}$ in Figure 2.)

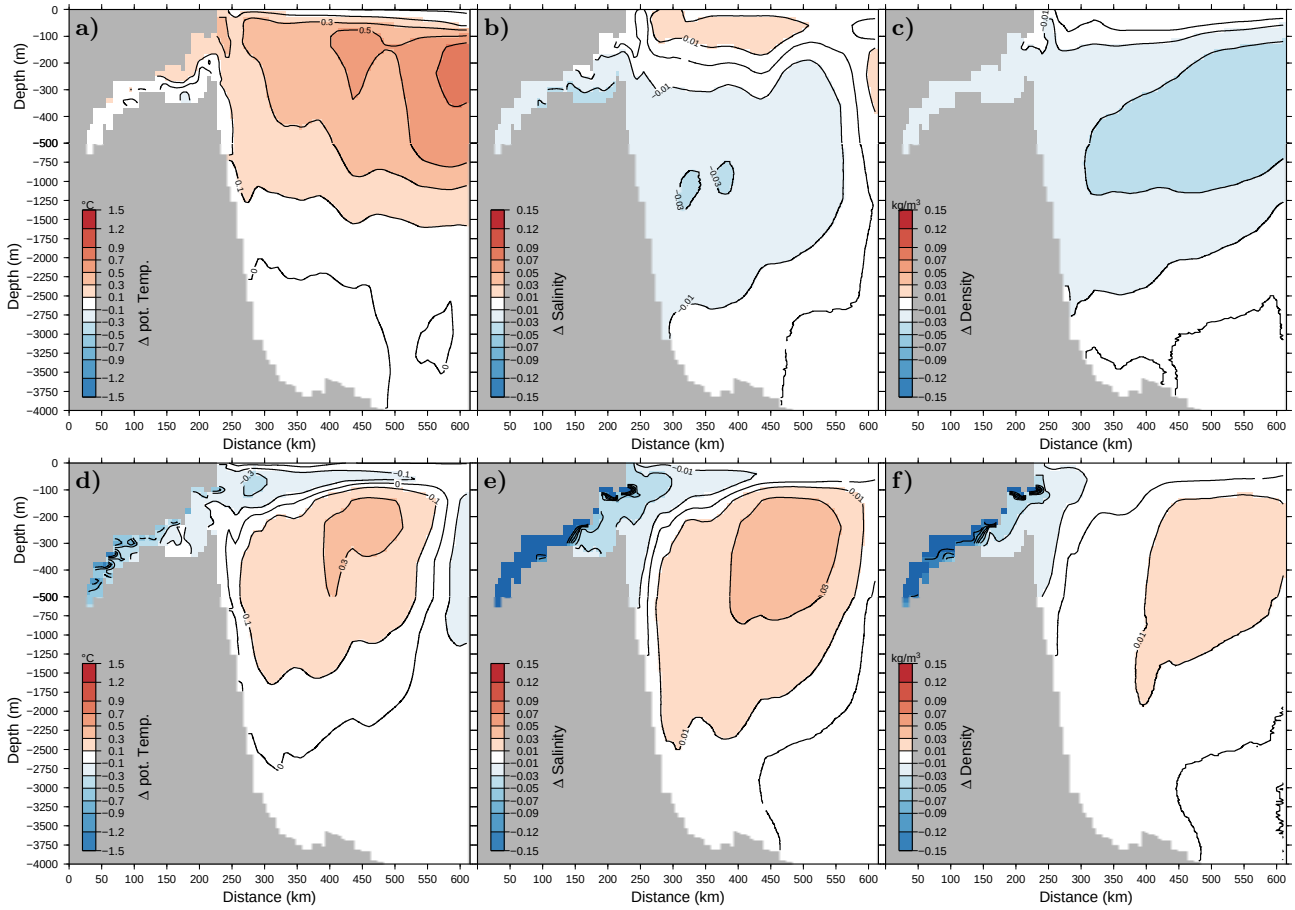

Fig. 7 Differences of temperature (left), salinity (middle), and density (right) between the following scenarios:
a–c): $\tilde{\mathcal{S}}^{\mathrm{inst}}_{1.0}$ and the corresponding "control run" (a–c). These anomalies represent the effect of the warming with suppressed ice-ocean interaction and correspond to arrow $\mathcal{B}$ in Figure 2.
d–f): The final states (after warming) of $\mathcal{S}^{\mathrm{inst}}_{1.0}$ and $\tilde{\mathcal{S}}^{\mathrm{inst}}_{1.0}$. These anomalies represent the effect of the ice-ocean interaction under warmed conditions and correspond to arrow $\mathcal{C}$ in Figure 2.

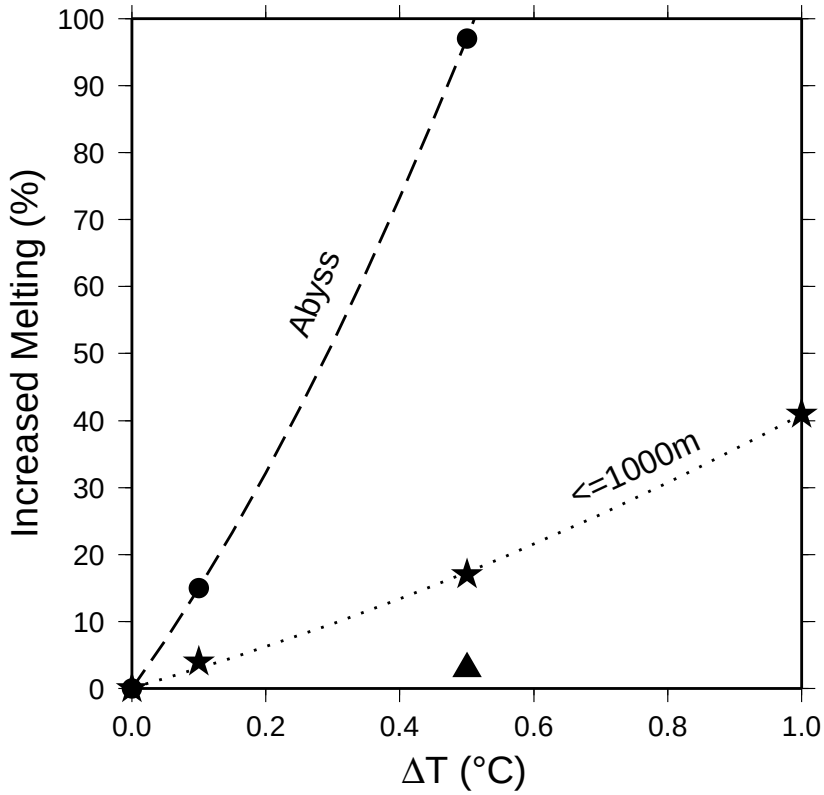

Fig. 8 Impact of increasing ocean temperatures on the melting of EWIS if the whole water column (dots, dashed line) or only the upper 1000 m (stars, dotted line) are warmed. The lines represent quadratic function fits as suggested by Holland et al. (2008). The black triangle indicates the lesser sensitivity of the FRIS to ocean warming of the upper 1000 m adapted from Thoma et al. (2006b).

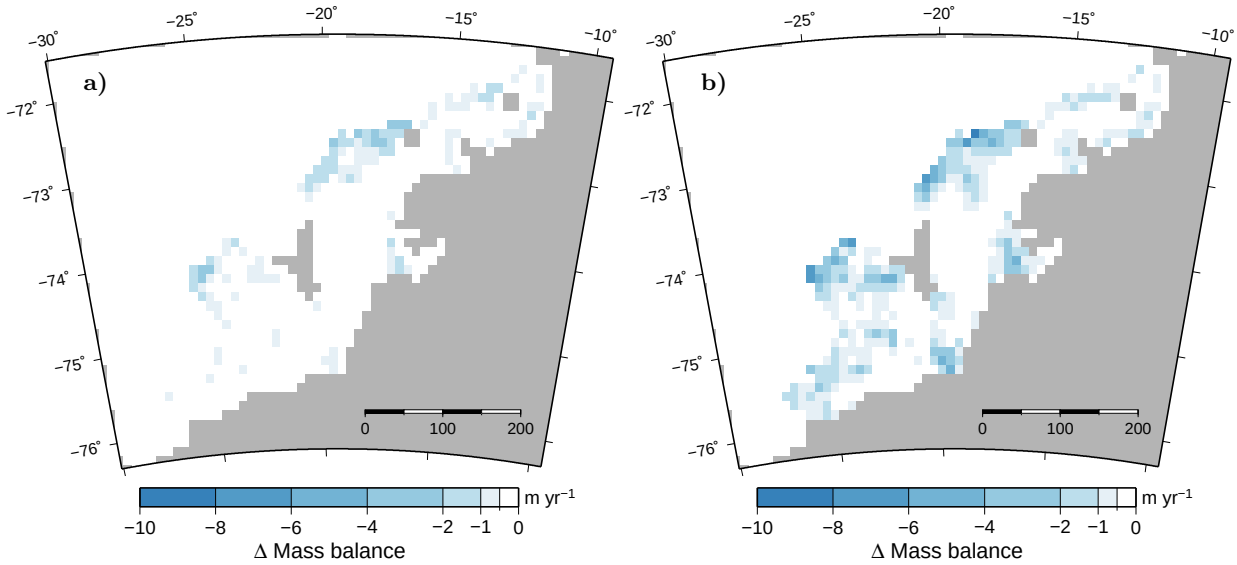

Fig. 9 Increased basal melt rate of EWIS as triggered by Scenarios ${}^{a}\mathcal{S}^{\text{inst}}_{0.5}$ (a) and $\mathcal{S}^{\text{inst}}_{1.0}$ (b), respectively. The differential values refer to the basal melt rate modelled for the control run (Thoma et al., 2006a).